Optics Communications 389 (2017) 181–188

Contents lists available at ScienceDirect

Optics Communications

journal homepage: www.elsevier.com/locate/optcom

Experimental demonstration of tri-aperture Differential Synthetic Aperture Ladar

Zhilong Zhao[a,b], Jianyu Huang[c], Shudong Wu[a,b], Kunpeng Wang[c], Tao Bai[a,b], Ze Dai[c], Xinyi Kong[a,b], Jin Wu[a,*]

[a] Institute of Electronics, Chinese Academy of Sciences, No. 19, North Fourth Ring West Road, Haidian District, Beijing 100190, China
[b] University of Chinese Academy of Sciences, No. 19, Yuquan Road, Shijingshan District, Beijing 100049, China
[c] Key Laboratory of Space Object Measurement, Beijing Institute of Tracking & Telecommunications Technology, Beijing 100094, China

ARTICLE INFO

Keywords:
Coherence imaging
Lidar
Synthetic aperture radar

ABSTRACT

A tri-aperture Differential Synthetic Aperture Ladar (DSAL) is demonstrated in laboratory, which is configured by using one common aperture to transmit the illuminating laser and another two along-track receiving apertures to collect back-scattered laser signal for optical heterodyne detection. The image formation theory on this tri-aperture DSAL shows that there are two possible methods to reconstruct the azimuth Phase History Data (PHD) for aperture synthesis by following standard DSAL principle, either method resulting in a different matched filter as well as an azimuth image resolution. The experimental setup of the tri-aperture DSAL adopts a frequency chirped laser of about 40 mW in 1550 nm wavelength range as the illuminating source and an optical isolator composed of a polarizing beam-splitter and a quarter wave plate to virtually line the three apertures in the along-track direction. Various DSAL images up to target distance of 12.9 m are demonstrated using both PHD reconstructing methods.

1. Introduction

Synthetic aperture ladar (SAL) technique has been progressed rapidly in recent decade [1–12]. Many laboratory-scale demonstrations or even an aerial-platform demonstration have verified the concept of producing image resolution beyond the diffraction limit of the real optical aperture. With laser as the active illuminating source, SAL could generate high resolution images of distant objects with a relatively small real optical aperture in a very short synthetic aperture time. A system of this type is very promising in space exploration.

SAL produces images by mathematically processing the Phase History Data (PHD) of the back-scattered laser signals from the object. Stable PHD is of pivotal importance in achieving high resolution images in a SAL system. Due to the short wavelength of laser illumination source, SAL is very sensitive to unknown motions of either the ladar or the target and to phase front distortions caused by atmosphere turbulence [13,14]. Tiny mechanical vibrations will generate enormous phase errors, corrupting the stability of PHD and seriously degrading the azimuth image resolution. As a result, compensating the pulse to pulse phase errors, whether by hardware or software techniques, is a requisite in forming high resolution images of any practical SAL.

Differential Synthetic Aperture Ladar (DSAL) is a hardware based technique to solve the problem of pulse-to-pulse phase error in SAL, which was proposed and patented by E. A. Stappaerts and E. T. Scharlemann in 2005 [15]. By utilizing two sub-apertures to receive the backscattered laser signals and calculating their differential phase in every azimuth shots, DSAL could remove pulse-to-pulse phase errors and reconstruct a stable azimuth PHD. Analytical and modeling studies showed that DSAL greatly relaxes both motion/vibration and laser spectral purity requirements [15].

The first DSAL experiment was reported by Z. W. Barber and J. R. Dahl in 2015 [16], where DSAL images of two simple cooperative targets at 1.83 m distance were demonstrated using a telecoms DFB laser with about 40 GHz chirped bandwidth and synthetic aperture length of 0.75 mm. In this paper, a stripmap mode DSAL setup with tri-aperture configuration using a linear-in-wavelength scanning laser in 1550 nm is introduced. High resolution images up to 12.9 m target distance are illustrated by using two different DSAL reconstruction methods.

2. Theoretical description on tri-aperture DSAL

The DSAL is set up with three sub-apertures. The geometry of the

* Corresponding author.
E-mail address: jwu909@263.net (J. Wu).

http://dx.doi.org/10.1016/j.optcom.2016.12.024
Received 20 June 2016; Received in revised form 7 December 2016; Accepted 8 December 2016

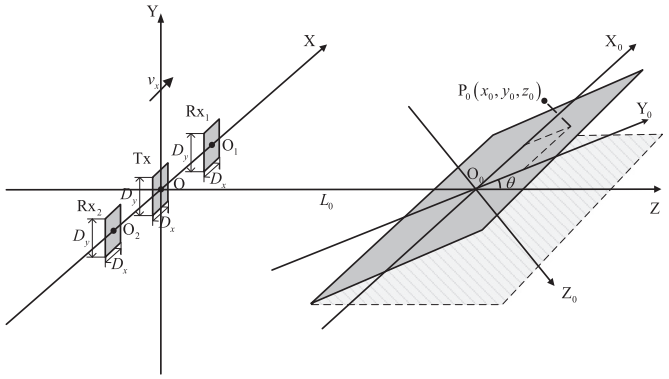

Fig. 1. Geometry of a tri-aperture DSAL.

tri-aperture configured DSAL is shown in Fig. 1, where the three sub-apertures are lined along the track with the center sub-aperture Tx for laser transmitting and the other two sub-apertures Rx_1 and Rx_2 for backscattered light receiving.

In Fig. 1, two sets of rectangular coordinates XYZ and $X_0Y_0Z_0$, referred to as the main coordinates and the target coordinates respectively, are established for the convenience of theoretical description, where two origins O and O_0 are L_0 spaced in line of sight (LOS) on the Z axis; the axis X and X_0 are paralleled to each other and the axis Y_0 and Z has an intersection angle θ. The three sub-apertures are assumed to all rectangular with the same size $D_x \times D_y$, and moving along the X axis with the same velocity v_x.

At azimuth sampling position X_m, the center positions of the three sub-apertures in the main coordinates can be set as follows

$$\begin{cases} \text{Tx:} & (X_m,\ 0,\ 0) \\ \text{Rx}_1\text{:} & (X_m + \Delta X_1,\ \Delta Y_1,\ \Delta Z_1) \\ \text{Rx}_2\text{:} & (X_m + \Delta X_2,\ \Delta Y_2,\ \Delta Z_2) \end{cases} \tag{1}$$

Where the two Rx apertures are assumed to have deviations (ΔX_i, ΔY_i, ΔZ_i) (i=1, 2) from the Tx aperture.

Under linear chirped laser illumination, the optical heterodyne detection signals obtained from two Rx apertures at the Tx aperture position (X_m, 0, 0) in Fig. 1 could be approximated as [17]:

$$\begin{aligned} &R_{1(2)}(X_m,\ t) \\ &\approx A_{1(2)} \iint T(x_0,\ y_0)dx_0dy_0 \cdot \exp\{-j\{2\pi f_0[t_{L1(2)} - \tfrac{2(L_{0m} + y_0\cos\theta) - \Delta Z_{1(2)}}{c} \\ &- \tfrac{(X_m - x_0)^2 + (X_m + \Delta X_{1(2)} - x_0)^2}{2cL_{0m}} - \\ &\tfrac{2y_0^2 + 2\Delta Y_{1(2)}(-y_0\sin\theta) + 2\Delta Z_{1(2)}(y_0\cos\theta) + (\Delta Y_{1(2)})^2 + (\Delta Z_{1(2)})^2}{2cL_{0m}}\Big] + \pi k \\ &\{[t_{L1(2)} - \tfrac{2(L_{0m} + y_0\cos\theta) - \Delta Z_{1(2)}}{c}][2t - t_{L1(2)} - \tfrac{2(L_{0m} + y_0\cos\theta) - \Delta Z_{1(2)}}{c}]\}\} \\ &\operatorname{sinc}\Big[\tfrac{D_x}{\lambda_0 L_{0m}}(X_m - x_0)\Big]\operatorname{sinc}\Big[\tfrac{D_x}{\lambda_0 L_{0m}}(X_m + \Delta X_{1(2)} - x_0)\Big] \\ &\operatorname{sinc}\Big[\tfrac{D_y}{\lambda_0 L_{0m}} y_0\sin\theta\Big]\operatorname{sinc}\Big[\tfrac{D_y}{\lambda_0 L_{0m}}(y_0\sin\theta - \Delta Y_{1(2)})\Big] \qquad t \in [0,\ \tau_{pul}^0] \end{aligned} \tag{2}$$

Where the subscript "1(2)" stands for the two apertures Rx_1 and Rx_2, respectively; and

$A_{1(2)}$ – constant for the two Rx apertures;
$T(x_0, y_0)$ – amplitude scattering coefficient at target surface point, diffusive scattering assumed;
$P_0(x_0, y_0, 0)$ – target point at the target coordinates (a plane target is assumed with z_0=0 for simplicity);
λ_0, f_0, k – the initial laser wavelength, frequency and chirp rate of the chirped laser signal, respectively;
$t_{L1(2)}$ –local signal delay time in the optical heterodyne detection of the two Rx aperture channels respectively;
L_{0m} – LOS distance assuming to depend on azimuth sampling position only;
$\tau 0$ *pul* – pulse length of optical heterodyne detection for SAL imaging.

Provided that the LOS distance remains constant during the synthetic aperture time, Eq. (2) shows that the PHD from both Rx apertures can form SAL images independently. However, as the LOS distance varies with the sampling position, enormous phase error will be generated from pulse to pulse, destroying the stability of PHD for azimuth aperture synthesis.

Eq. (2) also shows that the deviations of the aperture center positions affect the phase of the optical heterodyne detection signals differently. By very carefully setting the optics in the DSAL system, the following approximations can be reached

$$\begin{cases} |\Delta Y_i| \approx 0 \\ \Delta Z_1 \approx \Delta Z_2 \\ k[t_{L1} - \tfrac{2L_{0m} - \Delta Z_1}{c}] \approx k[t_{L2} - \tfrac{2L_{0m} - \Delta Z_2}{c}] \\ |k[t_{L1} - \tfrac{2L_{0m} - \Delta Z_1}{c}] - k[t_{L2} - \tfrac{2L_{0m} - \Delta Z_2}{c}]| << \tfrac{1}{\tau_{pul}^0} \end{cases} \quad (i = 1,\ 2) \tag{3}$$

Practically, the first two expressions in Eq. (3) could be achieved by properly setting the three sub-apertures and the last two ones are by both adjust the positions of the two Rx apertures and delay time of the two local signals for optical heterodyne detection.

With Eq. (3), Eq. (2) can be further expressed as

$$\begin{aligned} &R_{1(2)}(X_m,\ t) \\ &\approx A_{1(2)} \iint T(x_0,\ y_0)dx_0dy_0 \exp\left\{-j\left\{2\pi f_0\left[-\tfrac{(X_m - x_0)^2 + (X_m + \Delta X_{1(2)} - x_0)^2}{2cL_0}\right]\right\}\right\} \\ &\cdot \exp\{-j\{2\pi f_0[t_{L1(2)} - \tfrac{2(L_{0m} + y_0\cos\theta) - \Delta Z_{1(2)}}{c} - \\ &\tfrac{2y_0^2 + 2\Delta Y_{1(2)}(-y_0\sin\theta) + 2\Delta Z_{1(2)}(y_0\cos\theta) + (\Delta Y_{1(2)})^2 + (\Delta Z_{1(2)})^2}{2cL_0}\Big] + \pi k \\ &\{[t_{L1} - \tfrac{2(L_{0m} + y_0\cos\theta) - \Delta Z_1}{c}][2t - t_{L1} - \tfrac{2(L_{0m} + y_0\cos\theta) - \Delta Z_1}{c}]\}\} \\ &= A_{1(2)} \iint T(x_0,\ y_0)dx_0dy_0 \exp\left\{-j\left\{2\pi f_0\left[-\tfrac{\left(X_m + \frac{\Delta X_{1(2)}}{2} - x_0\right)^2 + \left(\frac{\Delta X_{1(2)}}{2}\right)^2}{cL_0}\right]\right\}\right\} \\ &\exp\{-j\{2\pi f_0[t_{L1(2)} - \tfrac{2(L_{0m} + y_0\cos\theta) - \Delta Z_{1(2)}}{c} \\ &- \tfrac{2y_0^2 + 2\Delta Y_{1(2)}(-y_0\sin\theta) + 2\Delta Z_{1(2)}(y_0\cos\theta) + (\Delta Y_{1(2)})^2 + (\Delta Z_{1(2)})^2}{2cL_0}\Big] + \pi k \\ &\{[t_{L1} - \tfrac{2(L_{0m} + y_0\cos\theta) - \Delta Z_1}{c}][2t - t_{L1} - \tfrac{2(L_{0m} + y_0\cos\theta) - \Delta Z_1}{c}]\}\} \end{aligned} \tag{4}$$

In Eq. (4), the sinc functions in Eq. (2) are omitted for simplicity and the following approximation is assumed

$$\frac{1}{L_{0m}} \approx \frac{1}{L_0} \tag{5}$$

Eq. (4) shows shat the target coordinates (x_0, y_0) contributes to the signal phases independently. By applying Fourier transformation in Eq. (4) with respect to fast time variable t, the range compressed image can be formed with a resolution of

$$\rho_{y_0} = \frac{c}{2k\tau_{pul}^0\cos\theta} \tag{6}$$

And the azimuth phase in Eq. (4) can be processed by two different PHD reconstruction methods according to standard DSAL theory [15].

Method I: Reconstruct the azimuth PHD by the following sampling equation

$$X_{m+1} - X_m = \frac{\Delta X_2 - \Delta X_1}{2} = \frac{\Delta X}{2} \tag{7}$$

where ΔX is the azimuth line distance between the two Rx apertures,